Hindawi Publishing Corporation
Journal of Nanomaterials
Volume 2014, Article ID 918607, 9 pages
http://dx.doi.org/10.1155/2014/918607

Research Article

Preparation and Characterization of Au/Pd Modified-TiO_2 Photocatalysts for Phenol and Toluene Degradation under Visible Light—The Effect of Calcination Temperature

Anna Cybula,[1] Grzegorz Nowaczyk,[2] Marcin Jarek,[2] and Adriana Zaleska[1]

[1] *Department of Chemical Technology, Gdansk University of Technology, 80-233 Gdańsk, Poland*
[2] *NanoBioMedical Center, Adam Mickiewicz University, Umultowska 85, 61-614 Poznań, Poland*

Correspondence should be addressed to Adriana Zaleska; adriana.zaleska@pg.gda.pl

Received 7 March 2014; Accepted 6 April 2014; Published 30 April 2014

Academic Editor: Arash Dehghan Banadaki

Rutile loaded with Au/Pd nanoparticles was prepared using a water-in-oil microemulsion system of water/AOT/cyclohexane followed by calcination. The effect of calcination temperature (from 350 to 700°C) on the structure of Au/Pd nanoparticles deposited at rutile matrix and the photocatalytic properties of Au/Pd-TiO_2 was investigated in two model reactions (toluene degradation in gas phase and phenol degradation in aqueous phase). Toluene was irradiated over Au/Pd-TiO_2 using light emitting diodes (LEDs, λ_{max} = 415 nm). The sample 0.5 mol% Pd/TiO_2 exhibited the highest activity under visible light irradiation in gas and aqueous phase reaction among all photocatalysts calcined at 350°C, while the sample modified only with gold nanoparticles showed the lowest activity. The Au/Pd-TiO_2 sample calcinated at 350°C possesses the highest photocatalytic activity when degrading phenol under visible light, which is 14 times higher than that of the one calcinated at 450°C. It was observed that increasing temperature from 350 to 700°C during calcination step caused segregation of metals and finally resulted in photoactivity drop.

1. Introduction

In the late 1980s, it was found that heterogeneous, composite, or sandwich colloidal metal particles have better efficiency than their corresponding single particles. Depending on the synthetic approach used in the preparation of bimetallic nanoparticles (BNPs), the distribution of each metal within a particle and their organization could adopt either core-shell, random alloy, alloy with an intermetallic compound type, or cluster-in-cluster or subclusters structures. Nanoparticles containing one or two noble metals were efficiently used both in catalytic [1, 2] and photocatalytic [3] reactions. Paalanen et al. have considered three key structural parameters, namely, (a) the size of the metal nanoparticles, (b) compositional variation between the two metals, and (c) the mixing pattern or nanostructure of the two metals that play a crucial role in determining the activity/selectivity and stability of bimetallic (e.g., Au-Pd) nanoparticle-based catalysts [4]. Thus, the ability to control nanoscale alloying and phase segregation properties is important for the exploration of the bimetallic nanoparticles for the design of advanced catalysts, photocatalysts, and other functional materials. The structure of bimetallic nanoparticles modified-semiconductor as well as their activity and surface properties can be modified by changing type of support, preparation conditions (TiO_2 source, type of reducing agent, and surfactant) [3], heat treatment temperature [5], atmosphere [6], metals content [7], preparation method [8], synergistic effect between two metals, and so forth. A combination of two or more kinds of metals has been widely applied in various materials to enhance the performance and reliability of the materials. Gold-palladium nanoparticles-based catalysts have been reported to be active for oxidation of benzyl alcohol [8–11], hydrogenation of 1-heptyne [12], oxidation of VOC [13, 14], oxidation of crotyl alcohol [15], CO oxidation [16], synthesis of hydrogen peroxide [17, 18], hydrodechlorination [19], and vinyl acetate synthesis [20]. There is a lot of information in the recent literature about the activity of Au/Pd-TiO_2 nanocomposites in catalytic reactions, however, only a few reports about the activity of these nanoparticles

in the photocatalytic reactions. Tanaka et al. successfully prepared Au-core Pd-shell particles supported on TiO_2 by a two-step photodeposition method. Samples were active in the photocatalytic dechlorination of chlorobenzene to benzene along with oxidation of 2-propanol to acetone under visible light irradiation [21]. It was shown that thickness control of the Pd shell is very important for both a satisfactory cocatalyst effect and absorption due to surface plasmon resonance (SPR) of Au nanoparticles [21]. Au-Pd alloy, supported on TiO_2, has been synthesized *via* a sol-immobilization method and successfully used for phenol oxidation under UV light [22]. Su et al. suggested that the metal nanoparticles can mediate undesired redox reactions that ineffectively consume photogenerated radicals, thus improving the photooxidation efficiency of phenol [22]. In this work, the effect of temperature calcination on the structure of Au-Pd nanoparticles deposited at rutile surface and photocatalytic activity of Au-Pd/TiO_2 nanocomposites under UV-Vis and visible irradiation was investigated. To our best knowledge, there has been no report on using visible light-emitting diodes (λ_{max} = 415 nm) for gas phase treatment over rutile loaded with Au/Pd nanoparticles. LEDs are a promising irradiation source, which allow reducing power consumption and costs of photocatalytic processes. The effect of the calcination temperature on photocatalytic activity in phenol degradation in aqueous phase and toluene degradation in gas phase as well as photocatalysts stability in two subsequent cycles was investigated.

2. Experimental

2.1. Materials and Instruments. Commercially available JRC-TIO-5 (mixture of rutile and anatase with majority of rutile, particle size: 570 nm, supplier: Catalysis Society of Japan) was used for the preparation of Au/Pd-TiO_2 photocatalysts. Palladium (II) chloride (5 wt.% in 10 wt.% HCl) and $HAuCl_4$ (Au ~ 52%) from Sigma-Aldrich were used as metal source in the preparation procedure. Cyclohexane, isopropyl alcohol, hydrazine, acetone, and AOT (dioctyl sulfosuccinate sodium salt) (POCH S.A., Poland) were used without further purification. Deionized water was used for all reactions and treatment processes.

DRS UV-Vis spectra of the synthesized materials were recorded in the scan range 200–800 nm using UV-Vis spectrophotometer equipped with an integrating sphere and TIO-5 was used as the reference. The crystal structure Au/Pd-TiO_2 was determined from XRD pattern measured in the range of $2\theta = 20–80^\circ$ using X-ray diffractometer with Cu target Kα-ray (λ = 1.5404 Å). Nitrogen adsorption-desorption isotherms were recorded at liquid nitrogen temperature (77 K) on a Micromeritics Gemini V (model 2365) and the specific surface areas were determined by the Brunauer-Emmett-Teller (BET) method in the relative pressure (p/p_0) range of 0.05–0.3. All the samples were degassed at 200°C prior to nitrogen adsorption measurements. The composition of the bimetallic NPs Au/Pd located at the TiO_2 surface was studied using Cs-corrected STEM (High Angle Annular Dark Field, HAADF) imaging supplemented with EDXS mapping.

2.2. Preparation of Photocatalysts. The monometallic Au and Pd-modified titanium (IV) oxide nanoparticles were prepared by adding gold or palladium precursor into water/AOT/cyclohexane *microemulsion A*. Surfactant AOT was used as a stabilizer for the nanoparticles into microemulsion system. Mixing of *microemulsion A* was carried out for 1 h under nitrogen and then gold and palladium were reduced by dropwise addition of *microemulsion B* containing the reducing agent (hydrazine) in the water phase. The molar ratio of the reducing agent to metal ions equaled to 3. Au-TiO_2 and Pd-TiO_2 was obtained by introducing powdered TiO_2 (TIO-5) into the microemulsion system containing metal nanoparticles. The water content was controlled by fixing the molar ratio of water to the surfactant. Figure 1 shows the images of microemulsions containing (a) Au^{3+} ions, (b) Au nanoparticles, and (c) Au modified TiO_2.

Microemulsion was mixed and purged with nitrogen for 24 h and then obtained precipitate was washed with acetone and water to remove the remaining surfactant, dried at 80°C for 48 h, and calcined in air for 2 h at different temperatures (with heating rate 2°C/min). Au/Pd-TiO_2 photocatalysts were received by the same method but with the addition of two metal precursors ($PdCl_2$ and $HAuCl_4$) into *microemulsion A*. Gold ions were introduced firstly followed by addition of palladium ions.

2.3. Measurement of Photocatalytic Activity in the Aqueous Phase. The photocatalytic activity of the Au-TiO_2, Pd-TiO_2, and Au/Pd-TiO_2 samples under the visible and UV-Vis irradiation was estimated by measuring the decomposition rate of phenol aqueous solution. Phenol was selected as a model pollutant because it is a nonvolatile and common contaminant present in industrial wastewaters. No degradation of phenol was observed in the absence of the photocatalyst or illumination. The aqueous phase contained 125 mg of the photocatalyst, 24 cm^3 of deionized water, and 1 cm^3 of phenol (C_0 = 500 mg/dm^3) as was described in our previous study [5]. The prepared suspension was stirred and aerated (V = 5 dm^3/L) for 30 min in the dark and then the content of the reactor was photoirradiated with a 1000 W Xenon lamp (Oriel) which emitted both UV and Vis irradiation. Measured light flux was (in the range from 310 to 380 nm) 68 mW/cm^2 for Xe lamp. The optical path included a water filter and a glass filter (GG 420) which cut off wavelengths shorter than 420 nm. During the irradiation the suspension (1 cm^3) was collected and filtered through syringe filters ($\varnothing$ = 0.2 μm) to remove the catalyst particles and then phenol concentration was estimated by the colorimetric method (λ = 480 nm) after derivatisation with diazo p-nitroaniline using UV-Vis spectrophotometer (DU-7, Beckman).

2.4. Measurement of Photocatalytic Activity in the Gas Phase. The photocatalytic activity of TiO_2 modified with Au, Pd, and Au/Pd nanoparticles in the gas phase reaction was determined by the toluene degradation process. In a typical measurement the suspension photocatalyst (0.1 g) in water was loaded as a thick film on a glass plate (3 cm × 3 cm) using painting technique. The obtained TiO_2-coated support was

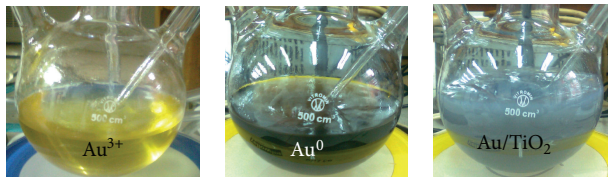

(a) (b) (c)

Figure 1: The images of (a) Au^{3+} ions, (b) Au nanoparticles, and (c) Au modified TiO_2 in the microemulsion water/AOT/cyclohexane.

dried and then placed at the bottom side of the photoreactor. The flat stainless steel reactor (V = 30 cm^3) was equipped with a quartz window, two valves, and a septa [23]. The gaseous mixture from a cylinder was passed through the reactor space for 1 min. The concentration of toluene in a gas mixture was about 100 ppm. After closing the valves, the reactor was kept in the dark for 15 min and then the content of the reactor was photoirradiated. As an irradiation source, an array of 25 LEDs (λ_{max} = 415 nm) was used. The analysis of toluene concentration in the gas phase was performed using gas chromatograph (Clarus 500, PerkinElmer) equipped with FID detector and Elite-5 capillary column as was described in our previous study [23].

3. Results and Discussion

3.1. BET Surface Area. Table 1 shows the sample label, BET surface, and pore size of Au, Pd, and Au/Pd modified-TiO_2 samples calcinated from 350 to 700°C. The surface area of the modified-TiO_2 samples, obtained by microemulsion system, fluctuated from 0.12 to 0.84 m^2/g and was dependent on the type/amount noble metal and calcination temperature. The samples modified with monometallic nanoparticles of palladium and gold (0.5 Pd/TiO_2 and 1.25 Au/TiO_2) had BET surface areas of about 0.214 and 0.198 m^2/g, respectively. The 0.5 Pd_1.25 Au/TiO_2 sample calcined at 350°C had the lowest BET surface area of about 0.12 m^2/g.

And the sample calcined at 700°C had the highest BET surface area of about 0.84 m^2/g. However, our previous studies have shown that as the calcination temperature increased, the BET surface area of Au/Pd-TiO_2 obtained by hydrolysis of TIP in the microemulsion system decreased progressively [5]. The surface area for pure nonmodified TiO_2 was 0.69 m^2/g. The pores size of obtained photocatalysts was very low and fluctuated from 0.0001 to 0.0003 cm^3/g.

3.2. UV-Vis Properties. DRS spectra of samples TiO_2 modified with monometallic (0.5% of Pd or 1.25% of Au) and bimetallic nanoparticles (0.5% of Pd and 1.25% of Au) are shown in Figures 2(a) and 2(b). The spectra were taken using pure TiO_2 (TiO-5, rutile) as a reference material. Obtained results indicated that the visible light absorption of the TiO_2 samples was significantly improved by introducing the gold and palladium nanoparticles. The absorption band edge is strongly related to gold and palladium nanoparticles size and shape presented in the photocatalyst samples. It can be seen that for sample 0.5 Pd/TiO_2 sharp absorbance edges occur at the wavelength of about 450 nm. For gold nanoparticles an increase in absorbance in the visible range at a wavelength of from 440 to 550 nm was observed, which is consistent with the LSPR of gold metal particles with the size in the nanometer range. For samples modified with Au/Pd nanoparticles and calcined at 350 and 400°C we observed a wide band from 550 to 750 nm for Au nanoparticles. Kowalska et al. showed that absorption at 560–610 nm was attributed to surface plasmon resonance (SPR) of larger Au nanoparticles (30–60 nm) [24]. In case of samples calcined at 700 and 450°C, we observed absorption peaks at ca. 440 nm, suggesting the presence of nanosize gold spherical particles and peaks at ca. 460 nm.

Mohamed and Baeissa showed that Pd-TiO_2 has an absorption sharp edge rising approximately 460 nm in the visible range, which is characteristic of surface plasma resonance corresponding to Pd particles [25]. The band at ~440 nm (2.84 eV) could also be attributed to the d-d transition of PdO particles, that is, to the presence of PdO bulk phase [26].

3.3. XRD Analysis. Figure 3 shows the results of X-ray diffraction measurements for the samples 0.5 Pd/1.25 Au-modified TiO_2 calcined from 350 to 700°C. Titanium dioxide is presented in two crystalline forms: anatase and rutile, but rutile was the main phase. The XRD peaks of anatase titania were detected at 25.2°. Typical diffraction peaks corresponding to rutile (2θ = 27.4°, 36.0°, 41.3°, 54.3°, and 56.6°) were observed in all the samples [12]. It can be seen that the intensity of the reflexes rutile and anatase increases with the calcination temperature. The XRD pattern of the sample calcined at 700°C reveals the highest reflexes intensities. The presence of a broad peak in the diffractograms of the bimetallic samples, centered at a value intermediate between the (1 1 1) peaks of metallic gold (2θ = 38.2°, 44.4°) and metallic palladium (2θ= 40.1°, 46.7°) indicated formation of Au/Pd alloy structure.

The diffraction peaks of 38.3° and 44.2° could be attributed to a gold-enriched alloy phase and the peaks of 40.2° and 46.4° to a palladium-enriched alloy phase. The crystallization occurs during the calcination. It can be seen that calcination temperature influences the intensity, the intensity ratio, and the width of the reflexes of Au/Pd. The diffraction Au/Pd peaks calcined at 700°C are sharp and intense, suggesting the aggregation of PdO particles to a certain extent during the oxidative thermal treatment [9].

Table 1: Sample label, BET surface area, and pore size of pure TIO-5, Au, Pd, and Au/Pd modified-TiO_2 samples calcinated from 350 to 700°C.

Sample label	Amount of noble metal precursor (mol.%)		Calcination temperature (°C)	BET surface area (m^2/g)	Pore size (cm^3/g)
	Pd	Au			
TiO_2 (TIO5-Rutile)*	0	0	—	0.69	0.0002
0.5Pd/TiO_2_350	0.5	0	350	0.21	0.0001
1.25Au/TiO_2_350	0	1.25	350	0.20	0.0003
0.5Pd_1.25Au/TiO_2_350	0.5	1.25	350	0.12	0.0001
0.5Pd_1.25Au/TiO_2_400	0.5	1.25	400	0.43	0.0002
0.5Pd_1.25Au/TiO_2_450	0.5	1.25	450	0.16	0.0001
0.5Pd_1.25Au/TiO_2_700	0.5	1.25	700	0.84	0.0004

*TIO-5: mixture of rutile and anatase with majority of rutile (particle size: 570 nm; supplier: Catalysis Society of Japan).

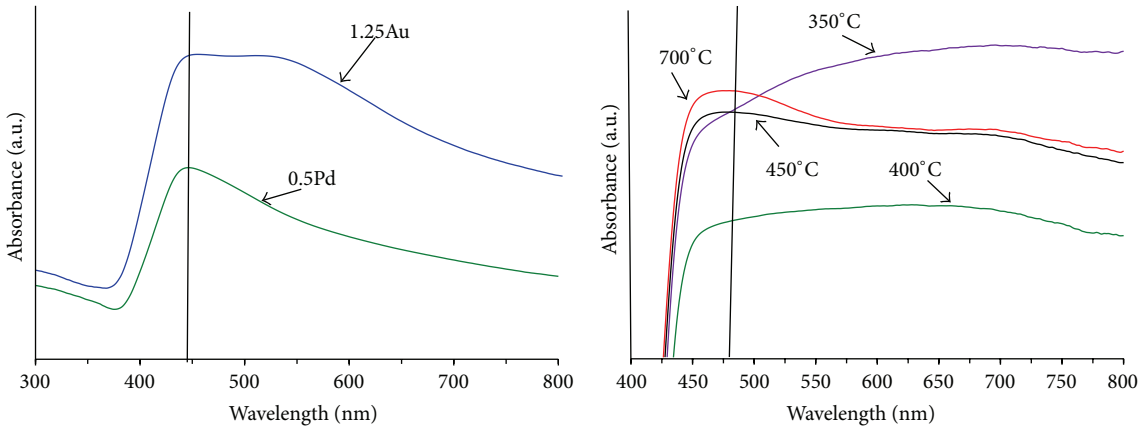

Figure 2: DRS spectra of samples (a) 0.5 Pd/TiO_2 and 1.25 Au/TiO_2 and (b) 0.5 Pd_1.25 Au/TiO_2 calcined at different temperature (from 350 to 700°C).

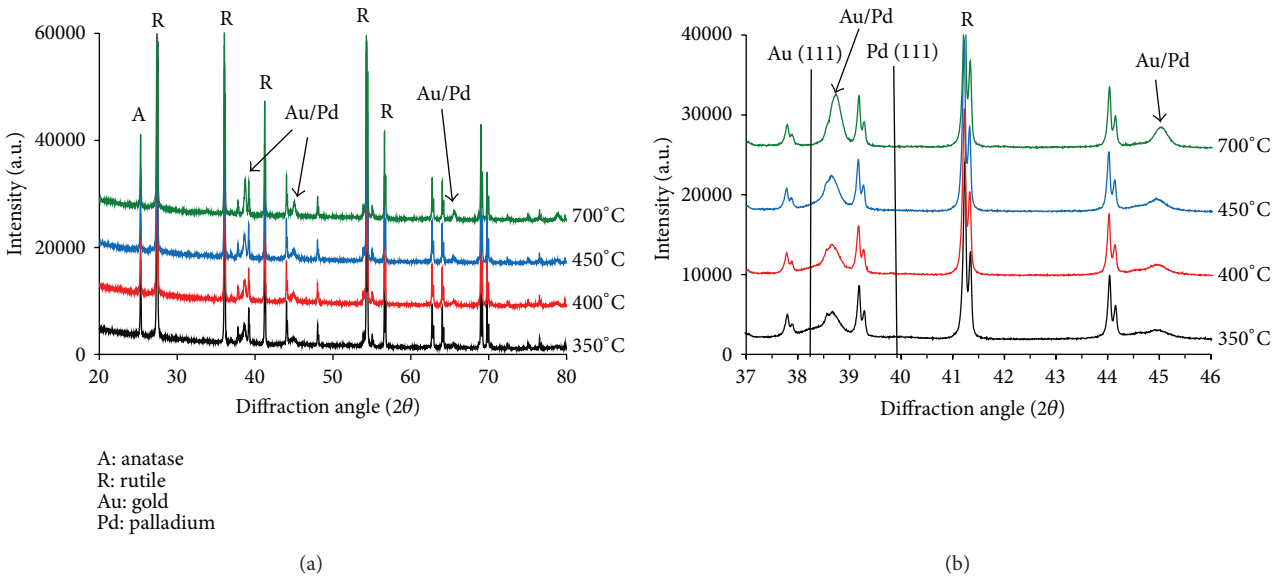

Figure 3: XRD pattern in ranges (a) 20–80° and (b) 37–46° of sample 0.5 Pd/1.25 Au-TiO_2 calcinated from 350 to 700°C.

3.4. Morphology. Gold and palladium are complete miscible that means all lattice planes which one could observe by TEM are in a range, for example, (111) between 0.23510 (Au) and 0.22517 nm (Pd), that makes it difficult to distinguish. Thus, the composition of Au/Pd nanoparticles was studied using Cs-corrected STEM (High Angle Annular Dark Field, HAADF) imaging supplemented with EDXS mapping. Most of the observed bimetallic nanoparticles Au/Pd, deposited at the TiO_2 surface, were in the range from 15 to 440 nm. The main fractions of Au/Pd nanoparticles calcined at 350°C had mostly spherical nanoparticles (in range from 65 to 180 nm) and longitudinal nanoparticles (about 98 and 250 nm). Figure 4 shows typical examples of nanoparticles calcined at 350 and 700°C, deposited on the surface rutile. For sample treated at 400°C, no nanoparticles smaller than 80 nm were found. Au/Pd nanoparticles about 440 nm had longitudinal shape and nanoparticles in the range from 80 to 195 nm had spherical shape.

Calcination at 450°C resulted in formation of mostly spherical 55–190 nm nanoparticles together with longitudinal 180 nm particles. For sample calcined at 700°C, spherical nanoparticles from 15 to 180 nm (mostly smaller) and particles about 290 nm with longitudinal shape were found. The morphology with mapping of bimetallic nanoparticles Au/Pd deposited at rutile surface is shown in Figure 5. The green spots were assigned to be Pd nanoparticles; the red spots were Au particles, whereas blue were Ti.

In case of the sample calcined at 350°C we observed that the gold content is higher than palladium content both in core and shell regions showing the alloy form. However, part of the palladium is not formed as nanoparticles. Figure 5(a) clearly shows aggregations of palladium located around the Au/Pd nanoparticles. Enhancement of the calcination temperature up to 400°C leads to migration of Pd into nanoparticles and fully alloying the metals. For sample treated at 400°C no aggregations of palladium located around the Au/Pd nanoparticles were found. In case of the sample calcined at 450°C it can be seen both types of nanoparticles structures, that is, core-shell and alloy. In the case of small nanoparticles (about 60 nm), it could be observed that the core of bimetallic NPs was rich in gold; however, the shell contained mostly palladium. However, bigger nanoparticles (about 150 nm) showed the alloy structure. Rising the calcination temperature to 700°C led to a fully alloyed system.

3.5. Photocatalytic Activity in Phenol Degradation. The photodegradation of phenol was performed in an aqueous solution under visible ($\lambda > 420$ nm) and UV-Vis light irradiation. Compared to pure TiO_2, TiO_2 modified with 0.5 mol% of Pd exhibited a significant increase in vis-driven phenol degradation reaction from 1.4 to 24% after 60 min irradiation (see details in Table 2). In case of the sample 1.25 mol% Au modified TiO_2 under visible light irradiation only 3.5% phenol was degraded after 60 minutes. The effect of temperature calcination on the photocatalytic activity of Au/Pd-TiO_2 in phenol degradation is presented in Figure 6 and Table 2. The highest photoactivity under visible light was observed for the sample calcined at the lowest temperatures of 350°C. The phenol degradation efficiency under visible light decreased from 22 to 13% for the sample calcined at 350 and 400°C, respectively. Further increase in annealing temperature resulted in a drop of photoactivity to 1.6% for the sample calcined at 700°C. In Figure 6(a) we can see that the samples calcined at 350 and 400°C have much higher activity than those calcined from 450 to 700°C. Our previous studies have shown that increasing temperature leads to photoactivity drop in photoactivity as well as the photocatalytic activity under visible light of samples Au/Pd-TiO_2 calcined at 350°C could be due to a high amount of carbon in the sample [5]. Concluding, the highest activity under visible light irradiation among all photocatalysts calcined at 350°C exhibited the sample 0.5 mol% Pd/TiO_2 nanoparticles (24%), while the lowest activity showed the sample modified with gold nanoparticles (3.5%). It was observed that modification of TiO_2 with bimetallic metals Au/Pd resulted in a slight decrease of photocatalytic activity as compared to 0.5 Pd/TiO_2, while a significant increase in photoactivity as compared to 1.25 Au/TiO_2 sample was noticed.

All samples modified with Au/Pd nanoparticles showed a high photoactivity under the influence of UV-Vis light; after 1 h of irradiation, 100% of phenol was degraded (see details in Table 2 and Figure 6(b)). The Au/Pd-TiO_2 photocatalysts calcined at 350 and 450°C showed the fastest degradation of phenol; degradation efficiency after 20 min of irradiation reached 100%. Compared to pure TiO_2, samples 0.5 Pd and 1.25 Au/TiO_2 exhibited the lower photoactivity under UV-Vis irradiation, as degradation efficiency after 60 min reached 89.2, 55.6, and 50.8%, respectively.

3.6. Photocatalytic Activity in Toluene Oxidation. Toluene photocatalytic degradation experiments were carried out under LEDs ($\lambda_{max} = 415$ nm) irradiation after 60 minutes, in two measurement cycles. All the as-prepared TiO_2 samples loaded with monometallic and bimetallic Au/Pd nanoparticles exhibited high photoactivity activity in gas phase. The sample 0.5 mol% Pd modified TiO_2 calcined at 350°C revealed the highest photocatalytic activity in toluene degradation. After 60 minutes of irradiation using LEDs ($\lambda_{max} = 415$ nm) after 1st and 2nd cycles of irradiation 79 and 78% of toluene were degraded. The sample 1.25 Au modified TiO_2 showed the lower average degradation (about 41%) compared to pure TiO_2 (about 58%). Further modification of TiO_2 with bimetallic metals Au and Pd (0.5 mol% Pd and 1.25 mol% Au calcined at 350°C) caused a decreased photoactivity as compared to 0.5 Pd/TiO_2, while an increase in photoactivity in toluene degradation as compared to 1.25 Au/TiO_2 sample. The toluene oxidation slight decreased in 1st cycle from 64 to 52% for the sample calcined at 350 and 450°C, respectively. Further increase in calcination temperature resulted in a slight increaseof photoactivity to 64% for the sample calcined at 700°C. The photoactivity decreased slightly in second measurement cycles which suggests that active sides of TiO_2 may have been blocked by toluene partial decomposition products, as was observed in our previous studies [23].

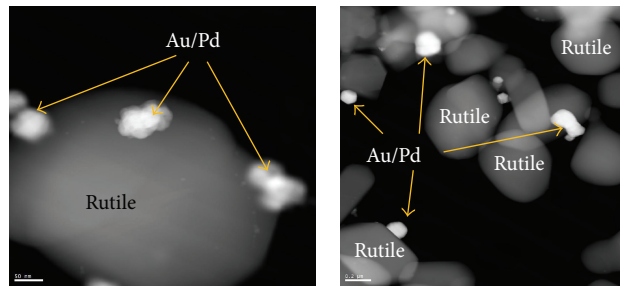

(a) (b)

Figure 4: High resolution HAADF images with z-contrast for Au/Pd nanoparticles calcined at (a) 350 and (b) 700°C.

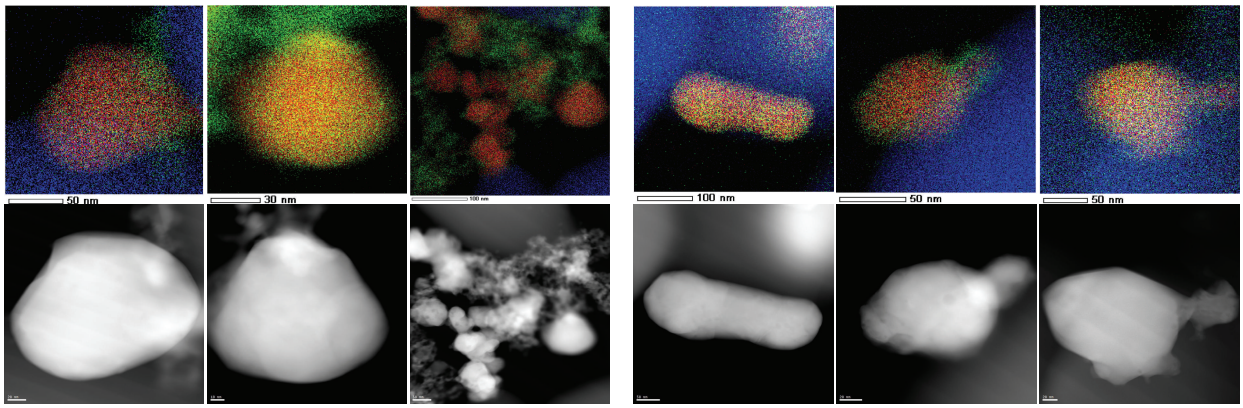

(a) 350°C (b) 400°C

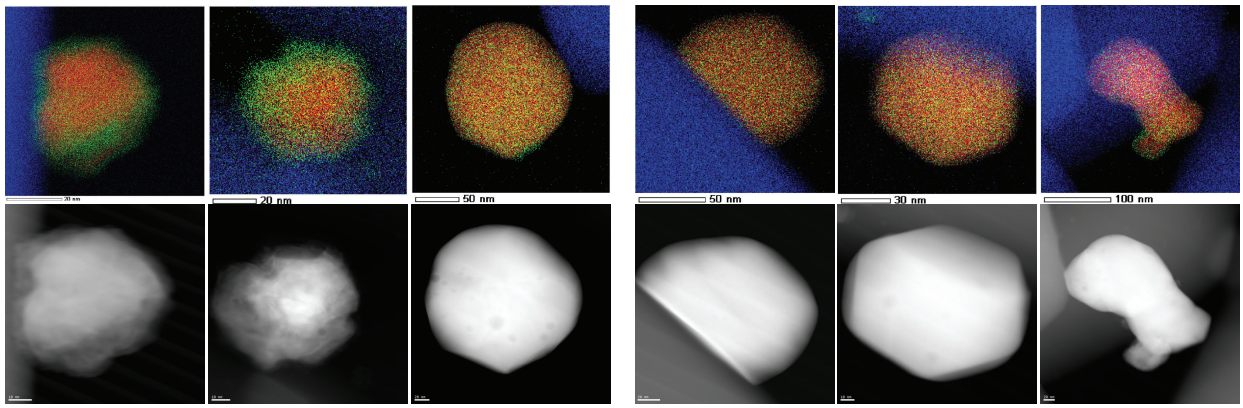

(c) 450°C (d) 700°C

Figure 5: HAADF images with z-contrast combined with mappings of Au/Pd nanoparticles deposited on rutile and calcined at (a) 350, (b) 400, (c) 450, and (d) 700°C (blue is Ti, red is Au, and green Pd).

Controlling the composition of metals within nanoparticles is difficult and far from straightforward. The mixing patterns of two metals are governed by various factors that include (a) preferential bonding of one metal with the stabilizer ligand/surfactant, (b) surface energy of the two metals, (c) sizes of the metals, and (d) the difference in the strengths of the hetero metal bonds and homo metal bonds [4]. Obtained results showed that sample calcined at 350°C exhibited nanoparticles that were alloys; however, the part of the palladium is not formed as nanoparticles. The calcination treatment at 400°C initiated fully migration of Pd into nanoparticles Au/Pd. Based on surface energy value it could be predicted that gold would be favored as surface material in a core-shell particle, since the surface energies of Au and Pd are 1.50 and 2.05 J/m^2, respectively [6]. However small nanoparticles calcined at 450°C supported at rutile surface have a core rich in gold, but the shell contained mostly palladium which finally resulted in photoactivity drop. This is in contrast to prediction based on surface energies of these two metals. It is thought that high calcination temperature

Table 2: Photocatalytic activity of pure TIO-5, Au, Pd, and Au/Pd modified-TiO_2 samples calcinated from 350 to 700°C in phenol and toluene degradation under UV-vis and Vis irradiation.

Sample	Efficiency of phenol degradation under UV-Vis after 60 min irradiation (%)	Efficiency of phenol degradation under visible light after 60 min. irradiation (%)	Efficiency of toluene degradation after 60 min. irradiation (%) LED (λ_{max} = 415 nm)	
			1st Cycle	2nd Cycle
TIO-5 Rutile	89.2	1.4	58	59
0.5Pd/TiO_2_350	55.6	24	79	78
1.25Au/TiO_2_350	50.8	3.5	42	40
0.5Pd_1.2Au/TiO_2_350	100	22	65	57
0.5Pd_1.2Au/TiO_2_400	100	13	54	50
0.5Pd_1.2Au/TiO_2_450	100	1.5	52	49
0.5Pd_1.2Au/TiO_2_700	100	1.6	64	60

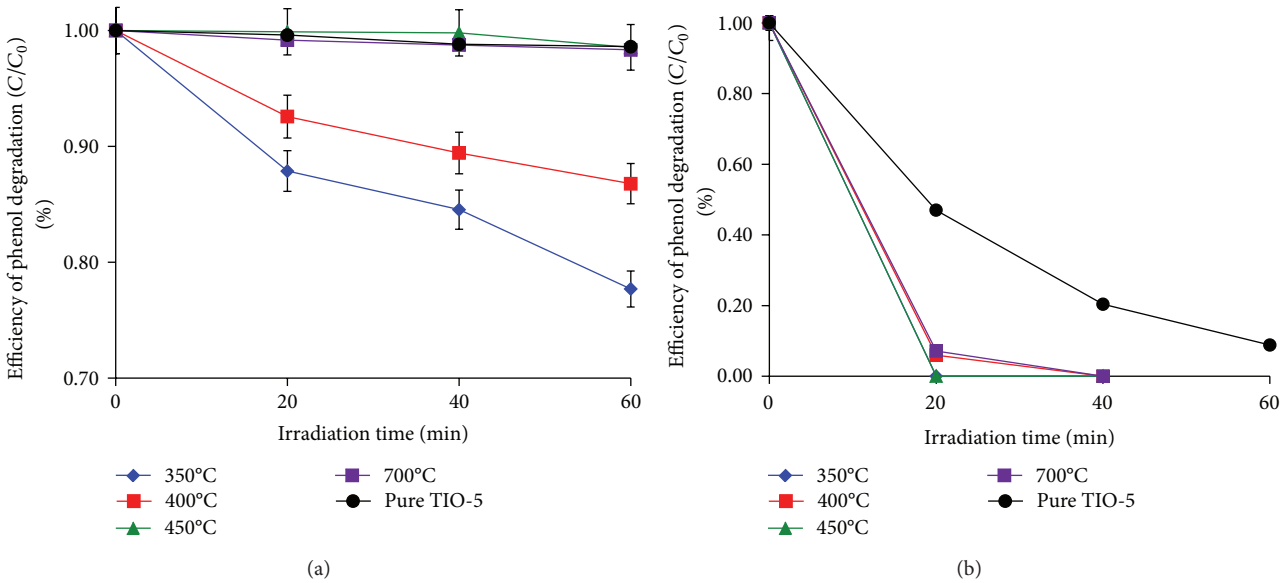

Figure 6: Kinetics of phenol degradation for sample 0.5 Pd_1.25 Au/TiO_2 calcined at different temperatures: (a) under visible light and (b) under UV-Vis light. Experimental conditions: light source: Xe lamp, $\lambda > 420$ nm, phenol initial concentration: 0.21 mM, m(TiO_2) = 125 mg, $T = 10$°C.

caused palladium readily oxidation to palladium oxide and segregates to the surface of the particle by the formation of Pd–O bonds [4]. Our previous results clearly showed that increase in calcination temperature (from 350 to 700°C) of Au/Pd nanoparticles deposited at anatase surface causes gold enrichment in the surface region. Moreover, Au/Pd nanoparticles deposited at anatase support and calcined at 350°C showed a gold-rich core and palladium-rich shell structure, whilst Au/Pd nanoparticles supported on rutile surface exhibited mostly alloys structure and part of the palladium is deposited separately. Thus, it is clearly shown that the structure of the bimetallic particles depends also on the type of support materials. Contrariwise to our results, Herzing et al. reported synthesis of Au/Pd particles in the form of homogeneous alloys; nevertheless, subsequent calcination in the air resulted in a progressive enrichment of Pd at their surface and a significant decrease in the activity of the catalyst [6]. Further increase in annealing temperature to 700°C in our results resulted in formation of homogenous alloys structures.

4. Conclusions

In summary, for the first time we have reported the effect of calcination temperature on photocatalytic activity under visible light in toluene and phenol degradation for rutile modified with Au/Pd monometallic and bimetallic nanoparticles. The sample 0.5 mol% Pd/TiO_2 exhibited the highest activity under visible light irradiation in gas and aqueous phase reaction among all photocatalysts calcined at 350°C, while the sample modified only with gold nanoparticles showed the lowest activity. The Au/Pd-TiO_2 sample calcinated at 350°C possesses the highest photocatalytic activity when degrading

phenol under visible light, which is more than 14 times higher than that of calcinated at 450°C. Enhancement in annealing temperature to 450°C resulted in increase of palladium concentration in the outer shell for small nanoparticles and in drop of photoactivity in phenol and toluene degradation under visible light. Further increase of temperature to 700°C caused slight increase in activity in the gas phase and no change in photoactivity in the aqueous phase under visible light irradiation probably due to formation of homogenous alloys structures.

Conflict of Interests

The authors declare that there is no conflict of interests regarding the publication of this paper.

Acknowledgments

This research was financially supported by National Science Centre, Poland (research Grant *Preparation and characteristics of novel three-dimensional semiconductor-based nanostructures using a template-free methods*, contract no. 2011/03/B/ST5/03243), and by National Centre for Research and Development, Poland (research grant *Nanomaterials and their application to biomedicine*, no. PBS1/A9/13/2012). The authors gratefully acknowledge Professor Stefan Jurga from NanoBioMedical Center for his support of this research.

References

[1] G. Ertl and H. Knoezinger, "Catalytic Process. Part B," in *Handbook of Heterogeneous Catalysis*, J. Weitkamp, Ed., vol. 4 and 5, Wiley-VCH, New York, NY, USA, 1997.

[2] J. Xu, H. Zhang, Y. Zhao et al., "Selective oxidation of glycerol to lactic acid under acidic conditions using AuPd/TiO_2 catalyst," *Green Chemistry*, vol. 15, p. 1520, 2013.

[3] A. Zielińska-Jurek, E. Kowalska, J. W. Sobczak, W. Lisowski, B. Ohtani, and A. Zaleska, "Preparation and characterization of monometallic (Au) and bimetallic (Ag/Au) modified-titania photocatalysts activated by visible light," *Applied Catalysis B*, vol. 101, no. 3-4, pp. 504–514, 2011.

[4] P. Paalanen, B. M. Weckhuysen, and M. Sankar, "Progress in controlling the size, composition and nanostructure of supported gold-palladium nanoparticles for catalytic applications," *Catalysis Science Technology*, vol. 3, p. 2869, 2013.

[5] A. Cybula, J. B. Priebe, M.-M. Pohl et al., "The effect of calcination temperature on structure and photocatalytic properties of Au/Pd nanoparticles supported on TiO_2," *Applied Catalysis B*, vol. 152-153, pp. 202–211, 2014.

[6] A. A. Herzing, A. F. Carley, J. K. Edwards, G. J. Hutchings, and C. J. Kiely, "Microstructural development and catalytic performance of Au-Pd nanoparticles on Al_2O_3 supports: the effect of heat treatment temperature and atmosphere," *Chemistry of Materials*, vol. 20, no. 4, pp. 1492–1501, 2008.

[7] A. Murugadoss, K. Okumura, and H. Sakurai, "Bimetallic AuPd nanocluster catalysts with controlled atomic gold distribution for oxidative dehydrogenation of tetralin," *The Journal of Physical Chemistry C*, vol. 116, pp. 26776–26783, 2012.

[8] J. A. Lopez-Sanchez, N. Dimitratos, N. Glanville et al., "Reactivity studies of Au-Pd supported nanoparticles for catalytic applications," *Applied Catalysis A*, vol. 391, no. 1-2, pp. 400–406, 2011.

[9] Y. Chen, H. Wang, C.-J. Liu et al., "Formation of monometallic Au and Pd and bimetallic Au-Pd nanoparticles confined in mesopores via Ar glow-discharge plasma reduction and their catalytic applications in aerobic oxidation of benzyl alcohol," *Journal of Catalysis*, vol. 289, pp. 105–117, 2012.

[10] C. Evangelisti, E. Schiavi, L. A. Aronica et al., "Bimetallic Gold-Palladium vapour derived catalysts: the role of structural features on their catalytic activity," *Journal of Catalysis*, vol. 286, pp. 224–236, 2012.

[11] P. G. N. Mertens, S. L. F. Corthals, X. Ye et al., "Selective alcohol oxidation to aldehydes and ketones over base-promoted gold-palladium clusters as recyclable quasihomogeneous and heterogeneous metal catalysts," *Journal of Molecular Catalysis A*, vol. 313, no. 1-2, pp. 14–21, 2009.

[12] B. Pongthawornsakun, S. Fujita, M. Arai, O. Mekasuwandumrong, and J. Panpranot, "Mono- and bi-metallic Au-Pd/TiO_2 catalysts synthesized by one-step flame spray pyrolysis for liquid-phase hydrogenation of 1-heptyne," *Applied Catalysis A*, vol. 467, pp. 132–141, 2013.

[13] M. Hosseini, T. Barakat, R. Cousin et al., "Catalytic performance of core-shell and alloy Pd-Au nanoparticles for total oxidation of VOC: the effect of metal deposition," *Applied Catalysis B*, vol. 111-112, pp. 218–224, 2012.

[14] M. Hosseini, S. Siffert, R. Cousin, A. Aboukaïs, Z. Hadj-Sadok, and B.-L. Su, "Total oxidation of VOCs on Pd and/or Au supported on TiO_2/ZrO_2 followed by "operando" DRIFT," *Comptes Rendus Chimie*, vol. 12, no. 6-7, pp. 654–659, 2009.

[15] A. F. Lee, C. V. Ellis, K. Wilson, and N. S. Hondow, "In situ studies of titania-supported Au shell-Pd core nanoparticles for the selective aerobic oxidation of crotyl alcohol," *Catalysis Today*, vol. 157, no. 1-4, pp. 243–249, 2010.

[16] Z. Suo, Ch. Ma, M. Jin, T. He, and L. An, "The active phase of Au-Pd/Al_2O_3 for CO oxidation," *Catalysis Communications*, vol. 9, no. 13, pp. 2187–2190, 2008.

[17] J. K. Edwards, S. J. Freakley, A. F. Carley, C. H. .J. Kiely, and G. J. Hutchings, "Strategies for designing supported gold-palladium bimetallic catalysts for the direct synthesis of hydrogen peroxide," *Accounts of Chemical Research*, vol. 47, no. 3, pp. 845–854, 2014.

[18] S. J. Freakley, M. Piccinini, J. K. Edwards, E. N. Ntainjua, J. A. Moulijn, and G. J. Hutchings, "Effect of reaction conditions on the direct synthesis of hydrogen peroxide with a AuPd/TiO_2 catalyst in a flow reactor," *American Chemical Society Catalysis*, vol. 3, pp. 487–501, 2013.

[19] L. A. Pretzer, H. J. Song, Y. -L. Fang et al., "Hydrodechlorination catalysis of Pd-on-Au nanoparticles varies with particle size," *Journal of Catalysis*, vol. 298, pp. 206–217, 2013.

[20] M. Chen and D. W. Goodman, "Promotional effects of Au in Pd-Au catalysts for vinyl acetate synthesis," *Cuihua Xuebao / Chinese Journal of Catalysis*, vol. 29, no. 11, pp. 1178–1186, 2008.

[21] A. Tanaka, K. Fuku, T. Nishi, K. Hashimoto, and H. Kominami, "Functionalization of Au/TiO_2 plasmonic photocatalysts with Pd by formation of a core-shell structure for effective dechlorination of chlorobenzene under irradiation of visible light," *The Journal of Physical Chemistry C*, vol. 117, pp. 16983–16989, 2013.

[22] R. Su, R. Tiruvalam, Q. He et al., "Promotion of phenol photodecomposition over TiO_2 using Au, Pd, and Au-Pd nanoparticles," *American Chemical Society Nano*, vol. 6, no. 537, pp. 6284–6292, 2013.

[23] M. Nischk, P. Mazierski, M. Gazda, and A. Zaleska, "Ordered TiO_2 nanotubes: the effect of preparation parameters on the photocatalytic activity in air purification process," *Applied Catalysis B*, vol. 144, pp. 674–685, 2014.

[24] E. Kowalska, O. O. P. Mahaney, R. Abe, and B. Ohtani, "Visible-light-induced photocatalysis through surface plasmon excitation of gold on titania surfaces," *Physical Chemistry Chemical Physics*, vol. 12, no. 10, pp. 2344–2355, 2010.

[25] R. M. Mohamed and E. S. Baeissa, "Preparation and characterisation of Pd-TiO_2-hydroxyapatite nanoparticles for the photocatalytic degradation of cyanide under visible light," *Applied Catalysis A*, vol. 464-465, pp. 218–224, 2013.

[26] K. Kocí, L. Matejová, M. Relia et al., "Sol-gel derived Pd supported TiO_2-ZrO_2 and TiO_2 photocatalysts;their examination in photocatalytic reduction of carbon dioxide," *Catalysis Today*, vol. 230, pp. 20–26, 2014.